

Dynamics of the cell-free DNA methylome of metastatic castration resistant prostate cancer during androgen-targeting treatment

Authors: Madonna R. Peter^{1,2}, Misha Bilenky³, Ruth Isserlin⁴, Gary D. Bader⁴, Shu Yi Shen⁵, Daniel D. De Carvalho^{5,6}, Aaron R. Hansen⁷, Pingzhao Hu⁸, Neil E. Fleshner⁹, Anthony M. Joshua^{7,10}, Martin Hirst^{3,11}, Bharati Bapat^{1,2*}

Affiliations:

1. Lunenfeld-Tanenbaum Research Institute, Sinai Health System, Toronto, Canada.
2. Department of Laboratory Medicine & Pathobiology, University of Toronto, Toronto, Canada.
3. Canada's Michael Smith Genome Science Center, BC Cancer Agency, Vancouver, Canada.
4. Terrence Donnelly Centre for Cellular and Biomolecular Research, University of Toronto, Toronto, Canada.
5. Princess Margaret Cancer Centre, University Health Network, Toronto, Canada
6. Department of Medical Biophysics, University of Toronto. Toronto, Ontario, Canada
7. Division of Medical Oncology and Hematology, Princess Margaret Cancer Centre, Toronto, Canada.
8. Department of Biochemistry and Medical Genetics, University of Manitoba, Winnipeg, Canada.
9. Departments of Surgery and Surgical Oncology, Division of Urology, University Health Network, Toronto, Canada.
10. Department of Medical Oncology, Kinghorn Cancer Centre, Australia.
11. Department of Microbiology and Immunology and Michael Smith Laboratories, University of British Columbia, Vancouver, Canada.

*Corresponding author: Dr. Bharati Bapat. 60 Murray Street, Toronto, ON, Canada, M1B 1Y5.

Telephone: 416-586-4800, Ext: 5175. Email: bapat@lunenfeld.ca

Abstract:

Background: Identifying treatment resistance in metastatic castration resistant prostate cancer (mCRPC) prior to initiating therapy would be a major asset in the clinical management of this highly aggressive and lethal form of the disease. As biopsy of metastatic lesions in this disease state is often not feasible, circulating cell free DNA (cfDNA) is an emerging tool to detect molecular drivers of resistance. While several studies have implicated the potential of mutation detection in cfDNA, DNA methylation changes have also shown promise as diagnostic and prognostic biomarkers in all stages of prostate cancer. Indeed, these tumor-derived DNA methylation patterns are detectable in circulation. However, the dynamics of the methylome in cfDNA has not been extensively studied, especially during treatment with current androgen-targeting agents.

Results: In this study, we performed genome-wide methylation sequencing analysis of cfDNA derived from mCRPC patients undergoing treatment with either Abiraterone acetate or Enzalutamide. Analysis of sequentially collected plasma cfDNA samples was performed, examining changes in the cfDNA methylome from prior to starting treatment (baseline), 12-weeks during treatment and upon clinical progression. We developed a comprehensive analysis pipeline to identify differentially methylated regions within each patient during treatment. We examined the frequency of genome wide cfDNA methylation changes across all patients and correlated these patterns with time to clinical progression. Overall, changes in well-established prostate cancer methylation markers and alterations in key pathways, such as Wnt and neuronal

development, were detectable in cfDNA. Patients that maintained methylation changes from baseline to week-12 and until progression tended to have a longer time to clinical progression (TTP). Importantly, we observed that markers associated with a highly aggressive form of the disease, Neuroendocrine-CRPC (NE-CRPC), could be detected prior to initiating treatment and were associated with a faster TTP.

Conclusions: Treatment-related methylation changes associated with TTP highlights the potential of monitoring cfDNA methylome during therapy in mCRPC. Our findings also suggest that detection of NE-CRPC associated methylation signatures in earlier stages of treatment may serve as predictive markers of response to androgen-targeting agents.

Key words: metastatic castration resistant prostate cancer, circulating cell free DNA, DNA methylation, epigenetic modifications, genome-wide methylation analysis

Background:

Prostate cancer (PCa) is the most common cancer and the second leading cause of cancer-related deaths among males (1, 2). Androgen deprivation therapy (ADT) to reduce systemic androgen levels continues to be the major treatment for aggressive PCa (3). While ADT is initially beneficial, treatment resistance leads to the most lethal form of PCa, metastatic castration resistant prostate cancer (mCRPC) (4). Despite castrate levels of systemic androgens, these tumors can continue to rely on the androgen receptor (AR) pathway to promote tumor growth and metastasis (5). Indeed, androgen-targeting agents, Enzalutamide and Abiraterone acetate, can improve overall and progression-free survival in both the pre- and post-chemotherapy settings (6-9).

Enzalutamide is an antiandrogen that directly inhibits full-length AR. Abiraterone inhibits CYP17A1, which catalyzes extragonadal androgen production (10, 11). Both treatments perform similarly to suppress the androgen pathway, and choice of treatment is often dependent on comorbidities (12). However, primary and eventual secondary resistance to Abiraterone or Enzalutamide remains an ongoing challenge. As a result, the treatment landscape of mCRPC is complex and continues to focus primarily on the order/sequencing of therapies. For instance, recent trials demonstrated early treatment with Abiraterone or Enzalutamide in the hormone-sensitive state could be beneficial (13-15). However, there is a diverse array of molecular drivers contributing to disease heterogeneity amongst mCRPC patients (16), leading to variable response to current treatment strategies. Therefore, reliable biomarkers are needed to facilitate optimal therapy sequences for each patient prior to starting treatments.

Liquid biopsies are emerging as a minimally invasive source of biomarkers, reflecting tumor turnover (17). This is particularly advantageous for mCRPC, as most patients have had prior radical prostatectomy and bone metastases are often inaccessible. Numerous studies have explored the potential of circulating tumor cell (CTC) or circulating nucleic acid markers in mCRPC (18). Counting the number of CTCs and/or characterization of molecular alterations (i.e. genomic and transcriptomic) are promising markers that capture tumor heterogeneity (19). For instance, increased CTC number is associated with poor prognosis, and expression of the ligand-independent AR-V7 splice variant by CTCs is associated with resistance to Enzalutamide and Abiraterone (20-22). However, low CTC counts prior to first-line treatment and the need for robust CTC surface markers for their optimal detection remain an ongoing challenge (23, 24). Furthermore, some AR-V7 positive patients may still benefit from androgen therapies, while

certain AR-V7 negative patients show variability in treatment response (25, 26). In addition, highly aggressive androgen-independent Neuroendocrine-CRPC (NE-CRPC) tumors express lower levels of AR-V7 than Adenocarcinoma-CRPC patients (27). Therefore, additional markers are needed to identify this subset of patients.

Circulating cell free DNA (cfDNA) can harbor tumor-specific somatic mutations and capture tumor heterogeneity (28). There is a high concordance (>90%) of tumor mutations (i.e. *AR*, *BRCA2*) between matched cfDNA and mCRPC biopsies (17). Although the proportion of circulating tumor DNA (ctDNA) can vary from 1-2% to ~30% of cfDNA in mCRPC, the sequencing throughput of massively parallel sequencing platforms can sample cfDNA with sufficient coverage (29). For instance, targeted sequencing of *AR* in cfDNA can detect mutations associated with resistance to Enzalutamide or Abiraterone (30, 31). However, genomic aberrations are not the only contributors to molecular and phenotypic heterogeneity in mCRPC. Aberrations in the epigenome are a hallmark of all stages of PCa, including DNA methylation alterations (32, 33). Hypermethylation in promoter regions of several genes, such as *GSTP1*, *APC*, *HOXD3* and *TBX15*, are currently being investigated as diagnostic and prognostic markers in earlier stages of PCa (33, 34). Furthermore, in biopsy tissue from metastatic lesions, distinct DNA methylation patterns were observed between NE-CRPC and Adenocarcinoma-CRPC (27).

CpG methylation can be detected from DNA extracted from tissue and various biofluids (35-37). Presence of promoter methylation in *GSTP1* and *APC* in cfDNA from mCRPC patients is prognostic of overall survival (35, 38). Using an array-based platform, differential cfDNA methylation patterns were observed between Abiraterone responsive versus resistant patients

(36). While these observations are promising, extensive genome wide analysis of the mCRPC cfDNA methylome during Enzalutamide or Abiraterone treatment has not been performed. Specifically, the changes/dynamics in the cfDNA methylome at various stages of treatment could help further delineate and predict response to current mCRPC treatments. Recently, genome-wide analysis using cell-free methylated DNA immunoprecipitation and high-throughput sequencing (cfMeDIP-seq) revealed tumor-specific methylation changes in cfDNA of patients with various cancers (39).

To identify circulating DNA methylation changes associated with response to either Enzalutamide or Abiraterone treatment, we monitored sequentially collected cfDNA samples from mCRPC patients, starting from prior to treatment initiation to eventual clinical progression, and performed comprehensive methylome assessment /analyses. We identified changes in key genes known to have altered methylation state in PCa. Pathway analysis of cfDNA methylome changes also reflected alterations in several oncogenic pathways, such as Wnt and neuronal development related genes. Importantly, we observed that methylation patterns in genes associated with NE-CRPC were correlated with time to clinical progression.

Results:

Study design and patient cohort

Tumor methylation signatures can be identified through comparison of cancer patients' cfDNA with either matched tumor tissue or healthy control cfDNA (39). In the case of mCRPC, biopsy of metastatic lesions in bone is not routinely feasible, and there is considerable molecular heterogeneity in this clinical state. Therefore, to identify methylation markers associated with

response to therapy, we opted for within/intra-patient differential methylation analysis. We hypothesized that sequential collection of cfDNA from visit A (baseline/pre-treatment) to visit B (week-12) to visit C (clinical progression) would reveal changes in the cfDNA methylome that reflect tumor responses, with each patient serving as their own internal control. As outlined in **Figure 1**, intra-patient comparison could potentially detect changes in abundance of methylated DNA fragments related to tumor response. For instance, loss of methylated fragments may reflect loss/reduction of tumor cells sensitive to treatment. In contrast, gains in methylated fragments could be associated with gains in treatment resistant tumor cells, since changes in methylome could occur due to non-tumor/treatment related changes. Therefore, our analysis entailed: (1) identification of intra-patient differentially methylated regions (**DMRs**) and (2) finding common genes/pathways with differential methylation, and establishing the frequency of these changes across all patients in this study.

We prospectively collected plasma from mCRPC patients receiving either Enzalutamide (n=12) or Abiraterone acetate (n=4) treatment. In total, 45 blood samples were collected and summarized in **Figure 2a**. Two Enzalutamide-treated patients were unable to provide Visit C samples (P2 and P26) and one Abiraterone-treated patient progressed prior to Visit B (P36). The majority of patients (14/16) presented with bone metastatic lesions upon mCRPC diagnosis, with a subset showing lymph node and soft tissue metastases (**Figure 2b**). Twelve patients demonstrated an initial favorable prostate-specific antigen (PSA) response ($\geq 50\%$ decline from baseline, **Figure 2c**), and most patients exhibited maximal PSA response (favorable or plateau) around Visit B (**Supplementary Figure 1**). Overall time to clinical progression (**TTP**) varied for

each patient, ranging from rapid/primary resistance to therapy to treatment-driven resistance following initial favorable response (**Figure 2d**).

Performance of cfMeDIP-seq strategy with PCa cell line DNA and cfDNA samples

We utilized an established cfMeDIP-seq approach, which was developed for low amounts of cfDNA and capable of ctDNA fractions as low as 0.001% (39). This technique was able to distinguish methylation patterns between various cancer types, including pancreatic, breast and colorectal cancer (39). Briefly, methylated cfDNA is enriched using an antibody specific for methylated CpG sites, followed by amplification of adapter-ligated libraries. For each sample, 10% of the DNA was reserved as an input control (without immunoprecipitation).

To benchmark this methodology for PCa samples, we generated a control from genomic DNA derived from PCa cell line, 22Rv1, sheared to the same size as cfDNA (**Supplementary Figure 2**). As an additional control, we spiked all samples with methylated and unmethylated *Arabidopsis thaliana* (AT) DNA, and confirmed increased recovery of methylated AT DNA (~80%) compared to unmethylated DNA (<0.06%) (**Supplementary Figure 2a**). Spiked AT DNA was added following sequencing adapter ligation to cfDNA and not detectable during sequencing. Increased enrichment of known methylated genes/regions in the genome of 22Rv1 cells, (40) including the *CDKN2A* gene body and the first exon of *TGFB2*, compared to the unmethylated promoter of *HOXD8* was confirmed (**Supplementary Figure 2b**).

We performed cfMeDIP-seq on all 45 samples collected. The average starting amount of dsDNA was 27 ng, and ranged from 9 to 50 ng, with no significant differences in cfDNA

amounts across visits and treatments (**Supplementary Figure 2c**). Following alignment and base quality filtering, 48-62% of the cfMeDIP reads and 80-85% of input control reads remained for DMR analysis (**Supplementary Figure 2d-e**). A majority of cfMeDIP-seq sequence reads aligned within gene bodies (major transcript starting from transcriptional start site/TSS to transcription termination site/TTS) and intergenic regions, as well as CpG Island (CGI), CGI shores, and TSS/promoter regions (TSS \pm 1.5Kb), together representing the entire genome (**Supplementary Figure 2f**). As expected, enrichment of methylated cfDNA in the MeDIP fraction over input control fraction was observed, especially within CpG rich regions. Similar distribution of regions was observed between Enzalutamide and Abiraterone treated patients (**Supplementary Figure 2 g-h**).

Intra-patient differential methylation analysis

To identify treatment-related differentially methylated regions (DMRs), we developed a DMR calling strategy for intra-patient analysis termed “cfDNA DMRHunter” (See **Supplemental methods** and **Supplementary Figure 3**). As location-specific cfDNA recovery sensitivity is unknown *a priori*, we used input control libraries to ensure uniform cfDNA read coverage across the whole genome. DMRHunter also uses the input controls to remove alignment artifacts from analysis. After filtering low quality and PCR duplicated reads, DMRHunter builds a background model and identifies differentially methylated CpGs (DMCs) across the genome. Adjacent DMCs with the same differential methylation state (UP or DOWN) were merged to identify DMRs with stringent z-score (>1.5), average read count (≥ 10) and false discovery rate (FDR = 0.01) cut-offs. There were a large number of DMRs across all comparisons and treatments, ranging from 93 000 to 154 000 DMRs (**Figure 3a**) with no

significant difference in median number of DMRs between comparisons and treatment (**Figure 3b-c**). The overall median DMR size was 74 bp, ranging from 2bp (single CpG sites) up to 4163 bp.

We next examined the directionality of these changes across comparisons. Conventionally, hypermethylation or hypomethylation is the typical terminology for methylation changes. However, for cfDNA, it is unclear whether these changes reflect a gain/loss of methylated CpGs at these specific genomic sites or changes in DNA fragment abundance, reflecting an altered cellular abundance contributing to the cfDNA pool. For our analysis we opted to define these DMRs as gains (UP) or loss (DOWN) in methylated fragments. There was no significant difference in the overall proportion of regions with increased or decreased methylation in all visit comparisons (**Figure 3d-f**) and between the treatment types for B vs A and C vs B (**Supplementary Figure 4a-d**). However, Enzalutamide-treated patients showed gains in the overall proportion of methylated cfDNA fragments in visit C compared to A (**Supplementary Figure 4e-f**). The majority of DMRs were found within gene bodies (protein coding and pseudogenes) and intergenic regions (**Figure 3g**). DMRs near/within transcription start sites (TSS)/promoters and CpG Islands (CGI), as well as non-coding RNA (ncRNA), were found, but with lower abundance. We chose to focus on DMRs within promoter and gene body regions, as CpG methylation changes in these locations are known to be associated with gene expression changes (41).

Methylation changes within promoter and gene body regions

The majority of DMRs within promoters (TSS +/- 1.5 Kb) were associated with protein coding (PC) genes, followed by long non-coding RNA (lncRNA), pseudogenes (Pseudo) and short non-coding RNA (sncRNA) regions (**Supplementary Figure 5a**). We observed minimal overlap among promoters of different gene/ncRNA categories, and overall distribution of DMRs in these regions did not vary between patients and visits (**Supplementary Figure 5b**). For all patients combined, the distribution of methylation changes within promoters (UP vs DOWN) did not vary significantly across most regions, with the exception of a slight increase in overall methylation in pseudogenes for C vs A (**Supplementary Figure 5c**). We focused on protein coding genes with at least one promoter DMR. Analyzing recurrence of these genes, we found that many of these genes were found in less than 5 patients for each comparison (**Supplementary Figure 5d-f**). We examined the most common protein coding genes (with DMRs in ≥ 5 patients) and found many genes overlapping across visit comparisons (**Figure 3h**), with the majority shared between Abiraterone and Enzalutamide groups. The most common genes showing either increases or decreases in promoter methylation are in **Supplementary Figure 6**, with certain genes implicated in PCa or other cancers. For instance, pyrroline-5-carboxylate reductase 1 (*PYCR1*), which is involved in proline biosynthesis and can promote tumor cell growth (42), often demonstrated gain of methylation at visit C.

We next performed pathway enrichment analysis for gene sets, which showed increased or decreased methylation in promoters during treatment (**Supplementary Figure 7 and 8** respectively). Variability in the types and frequency of pathways identified was observed across patients; however, cancer-related pathways such as Wnt and PI3K signaling were observed, with

neuronal pathways being the most frequent. Several promoter associated DMRs were only found among Enzalutamide-treated patients (**Figure 3h and Supplementary table 2**). The most frequently (6-7 patients, 20 comparisons) differentially methylated promoter region within the Enzalutamide cohort was *FGFR1*, which is overexpressed in PCa and implicated in metastasis (43).

We also examined the distribution of DMRs within gene bodies/known transcripts. The majority of these DMRs were associated with protein coding gene bodies across (**Supplementary Figure 9a-b**). Overall changes in methylation levels (UP vs DOWN) for these key regions did not change across comparisons (**Supplementary Figure 9c**). In contrast to promoter DMRs, many genes with body DMRs were shared across patients (**Supplementary Figure 9d-f**). Similarly, we focused on commonly altered gene bodies and found extensive overlap between visit comparisons and treatments (**Figure 3i**). We further examined net methylation change across these genes by scoring the ratio of increased to decreased methylation within each gene body, excluding genes that had no net change (i.e. equal number of UP and DOWN trends). We found 91 genes that were commonly altered across all comparisons (**Supplementary Figure 10**). In most cases, regardless of visit comparison, the methylation pattern for these genes clustered closely for the same patients. One such group of genes with increases in methylation at Visit C included *NFATC1*, which can promote tumorigenesis (44), and a histone deacetylase, *HDAC4*. While several Enzalutamide-specific genes were found (**Supplementary table 3**), common pathways including several differentiation-related and neuronal pathways were found among gene-body associated DMRs (**Supplementary Figures 11 & 12**),

PCa associated methylation changes in cfDNA

Aberrations in the DNA methylome is a hallmark of both androgen dependent PCa and mCRPC. Genomic DNA extracted from primary PCa tumors can harbor recurrent hypermethylation in gene promoters, including *GSTP1*, *TBX15*, *AOX1* and members of the HOX family of transcription factors (33). We assessed the overall promoter methylation status of genes that have been established as differentially methylated in PCa (**Figure 4a**). Among the most common differentially methylated gene promoters were genes involved in tumorigenic processes, such as *RUNX3*, *RGS12* and *FBP1*, with several differentially expressed in NE-CRPC (27), including the neuronal transcription factor *PHOX2A* (45) and a regulator of apoptosis, *CTBP2* (46). Similarly, several differentially methylated and cancer-related genes were found (**Supplementary Figure 13**), such as a master regulator of AR and driver of NE-CRPC, *ONECUT2* (47).

DMRs in genes associated with diagnosis and prognosis could reflect tumor cell response to treatments. While differential promoter methylation events in the well-established PCa-specific hypermethylated gene, *GSTP1*, were infrequent (**Figure 4b**), decreased gene body methylation coinciding with treatment response (i.e. PSA reduction) was shown in some patients (i.e. P3). Similar methylation regions were also observed in the PCa cell line LNCaP (48). Similarly, changes in *TBX15* methylation (1st intron) were associated with response to treatment (i.e. PSA) in certain patients (**Figure 4c**). While promising, there were no consistent DMRs in these genes that could classify patients by androgen-targeting treatment response. A caveat is that many of these methylated genes were reported in earlier stages of PCa and may not reflect the changes in mCRPC.

To find potential “treatment sensitive” CpG sites in the genome, we next examined differentially methylated CpG sites (DMCs) among patients that completed all study visits, specifically CpG sites that fluctuated in ≥ 2 visit comparisons. DMCs were analyzed as DMR size for similar genomic regions varied within and across patients. We stratified the proportion of DMCs that were uniquely found in single visit comparisons and those shared across all visits (**Figure 5a**). We identified DMCs present in two or more visit comparisons for each patient and associated them with gene promoters and bodies. Analysis of gene promoters containing DMCs revealed minimal overlap amongst patients, with P4, P31, P38 and P3 showing the highest overlap of 8 shared genes: *NPBWR1*, *ZSCAN12*, *PCDHGA11*, *PHOX2A*, *TBX10*, *TEX28*, *TKTL1* and *TSPAN32* (**Supplementary Figure 14a**). In contrast, we observed a high degree of overlap amongst patients when looking at DMCs within gene bodies, with the exception of P3 (**Supplementary Figure 14b**). Interestingly, we also noted a positive correlation between the proportion of DMCs shared across all visits and TTP (**Figure 5a**).

We examined 3 major combined scenarios observed among 14 total: (1) scenarios 7 and 8, increase/decrease in methylation in visit C vs B or A (**Figure 5a**); (2) scenarios 9 and 10, increase/decrease in B and C vs A; (3) those that go up or down in B vs A and then return to same levels in C (13 & 14). The proportion of these three combined scenarios was correlated with time to progression (TTP), and we found that those patients with more DMCs that increased/decreased at visit B and maintained at visit C (scenarios 9 and 10) had a longer TTP (**Figure 5b**). Although scenarios 7 & 8 did not correlate with TTP, those patients with a higher proportion of scenarios 13 & 14 had a possible trend towards faster TTP (**Supplementary figure**

14 c-d). This suggests that genome-wide cfDNA methylation dynamics can reflect response to treatment in mCRPC patients.

Neuroendocrine-CRPC related cfDNA DMRs

As many of the DMRs were associated with genes implicated in several neuronal pathways and differentiation, we integrated cfDNA DMRs with those identified from biopsy samples from NE-CRPC versus Adenocarcinoma-CRPC in an independent mCRPC patient series (27). While this published dataset utilized reduced representation bisulfite sequencing (RRBS), which primarily covers CpG rich regions (i.e. CGIs), several of these DMCs were found within cfDNA DMRs (29 355 CpG sites out of 84 930 in NE-CRPC). In order to assess whether changes in these regions at earlier time points are associated with overall response to androgen-targeting agents, we examined the overlap between DMRs from the A vs B comparison and NE-associated DMRs. As P36 progressed prior to visit B (**Figure 2d**), we included this patient in the analysis (examining A vs C). In this case, we examined the changes in methylation from the perspective of visit A. That is, increased methylation in visit A vs B/C (UP in A) or decreased methylation in visit A (DOWN in A). We proposed that the abundance of methylated cfDNA fragments from certain regions may reflect key genes/regions to monitor prior to initiating therapy. The overall proportion of these DMRs that were increased or decreased in methylation at A vs B (or C for ID 36) varied across the patients (**Figure 6a**). Interestingly, we noted that these DMRs (A vs B) appeared to be related to TTP. We examined the ratio of DMRs containing NE-CRPC associated CpG sites with more methylated fragments in Visit A to those with less methylation. In order to further delineate key regions, we applied various FDR thresholds to these DMRs to examine the effect on correlation with TTP (**Figure**

6b). We found an optimal set of regions that were negatively correlated with TTP: that is, the more methylated cfDNA fragments containing these NE-CRPC associated CpGs, the faster/shorter the TTP (**Figure 6c**). To determine whether the amount of NE-CRPC related methylation patterns at visit A was associated with a faster TTP, we performed ROC analysis for various TTP cut-offs (ranging from ≤ 20 to 35 weeks). We found that an increased ratio of NE-CRPC DMRs UP in visit A can stratify patients that progressed as early as 25-weeks (area under the curve, AUC: 0.927, CI: 0.773-1) (**Figure 6d**). These sites may serve as potential predictive markers of resistance to androgen-targeting agents.

Discussion

In this study, we showed that methylome analysis of the cfDNA from mCRPC patients can capture treatment-related epigenetic alterations. We found changes in well-established PCa methylation markers associated with response to treatment. Importantly, we demonstrated that cfDNA contains NE-CRPC related methylation signals, which have the potential to be utilized as predictive markers of treatment response. Methylation of several oncogenic driving pathways were detected in cfDNA across time points, suggesting that methylome analysis of patients' liquid biopsies can serve as a monitoring tool during treatment, as well as highlight potential targets for future therapies.

A key advantage of liquid biopsy-based versus tissue-biopsy approaches is the ability to capture tumor heterogeneity. To date, much focus has been placed on genomic alterations, which can help identify *AR* mutations related to resistance to Abiraterone/Enzalutamide (30, 31). However, few studies have highlighted that cfDNA methylation markers may help further

stratify patients (35, 36). In a recent study of 600 mCRPC patients receiving docetaxel, increased methylated *GSTPI* at baseline was associated with longer overall survival, and loss of methylation after two cycles of treatment corresponded with longer time to PSA progression (49). Furthermore, patients that exhibited loss in methylated *GSTPI* after two cycles of treatment had better overall survival. In this study, we observed some cases in which there were losses of *GSTPI* methylation in certain treatment responsive patients (PSA reduction). We also examined other tissue-based methylation markers (promoter and gene body), including *TBX15* and *RUNX3* (33), and similar heterogeneity amongst patients was observed. This in part could be explained by differing mechanisms between docetaxel and androgen-targeting agents. Due to intra- and inter-tumor heterogeneity (50, 51), androgen targeting agents may not target all androgen-independent tumor cells which could also harbor these methylation markers. Furthermore, most well-studied methylation markers were derived from earlier stages of PCa, whereas further epigenomic instability is known to occur with the mCRPC state (52).

A unique strength of our study is the sequential analysis using a genome-wide approach, which highlights progressive changes in genes involved in tumorigenic processes in PCa and other cancers. Commonly altered genes in the promoter region included *PYCR1* and *SHARPIN*, which are known to be upregulated in PCa tissue and involved in processes such as proliferation and angiogenesis (53). Gene body methylation was observed in *NFATC1*, *HDAC4*, *PHOX2A*, *CTBP2*, and master regulator of NE-CRPC, *ONECUT2* (44-47). Pathway analysis also further highlighted key mechanisms that have been established in prostate tumor tissue studies, including the wnt pathway (16). Interestingly, the methylation patterns amongst these genes demonstrated extensive variability across patients and visits. In order to further delineate key

regions, we further assessed common regions that changed during treatment. These changes appeared to reflect dynamics of treatment response. For instance, patients that demonstrated CpG changes (up or down) in visit B and sustained the changes by visit C appeared to have a longer TTP. In contrast, there was a trend towards shorter TTP amongst patients that did not demonstrate sustained methylation changes. Among the genes included was Neuropeptides B/W receptor 1 (*NPBWR1*), which was shown to be upregulated in basal cells from prostate tissue (54), thus highlighting that genome-wide cfDNA methylation analysis is able to capture tumor dynamics and may further have additive potential to mutation analysis.

We also observed that many of the differentially methylated genes overlapped between Enzalutamide- and Abiraterone-treated patients. Although there are ongoing studies to compare efficacy of either treatment (55), the current consensus is that both perform similarly, and deciding between treatments in a patient-specific manner remains an ongoing challenge. We identified sets of genes altered in the promoter and gene body locations, including one large set amongst Enzalutamide treated patients. We were limited by the number of Abiraterone-treated patients, which may have limited heterogeneity, as seen in the larger Enzalutamide cohort. Further studies are needed to examine if the methylome is different between these treatment types. However, similar pathways were observed between the treatments, with neuronal pathways being the most prominent.

Given these neuronal-related genes/pathways, we wanted to examine the utility of these methylation changes in helping to predict treatment outcome, especially in identifying Neuroendocrine-CRPC. With our unique study design of sequential sampling, we could detect

these methylation trends at earlier time points, demonstrating that the proportion of Neuroendocrine-like DMRs correlated with faster/shorter time to progression. In particular, the higher the proportion of certain DMRs with these NE-CRPC associated methylation patterns, the faster the time to progression. While we did not have confirmatory biopsies or other markers of NE disease (i.e. chromogranin A), increased methylation at Visit A could be utilized as predictive markers of response to androgen-targeting agents. Although we are currently limited to a single cohort, we now have a set of candidate regions that could be validated in additional cohorts.

Conclusions

Our genome-wide sequencing protocol and analysis strategy has demonstrated the utility of intra-patient monitoring of cfDNA methylation. If changes in the methylome during treatment were sustained until clinical progression, these patients appeared to have a better prognosis with androgen-targeting treatment. Interestingly, methylation patterns associated with a highly aggressive form of the disease may serve as potential predictive markers. Further independent validation of these markers is needed to assess this predictive potential.

Methods

Patient cohort

All patients in this study were recruited from the Princess Margaret Cancer Centre Genitourinary Clinic, and informed written consent was obtained in accordance with approved institutional Research Ethics Board protocols from University Health Network (UHN) and Sinai Health System (SHS). The UHN Genitourinary Biobank performed patient recruitment, blood

collection and clinical follow-up. All patients were chemotherapy naïve and developed resistance following initial PCa treatments (local therapies and ADT) (**Supplementary Table 1**). A total of 12 Enzalutamide-treated (160 mg daily) and 4 Abiraterone-treated patients (1000 mg daily + Prednisone/Dexamethasone) completed study visits for cfDNA methylome analysis. Blood was collected at three time points: prior to starting treatment (**Visit A**), at 12-weeks during treatment (**Visit B**) and upon clinical progression/treatment change (**Visit C**). While we aimed to collect Visit B around week-12 (+/- 2 weeks), average time from baseline for Visit B was 12.7 weeks (ranging 9 - 17 weeks). Serum PSA levels were obtained throughout treatment, and the lowest PSA level (nadir) was used to determine PSA progression. Clinical progression was determined by several factors, including radiological evidence of additional/worsening metastases and symptomatic changes as assessed by the treating physician.

Blood sample processing and cfDNA isolation

Blood was collected at each time point in citrate cell preparation tubes (BD Biosciences, San Jose, CA, USA) and samples were processed within 2 hours from collection. Plasma was separated from peripheral blood mononuclear cells (PBMCs) by centrifugation at 1800 x g for 20 minutes. Isolated plasma was divided into 1 mL aliquots and stored at -80°C. Prior to cfDNA isolation, frozen plasma samples were rapidly thawed at 37°C and spun at 16 000 x g for 5 minutes. For each visit, we utilized 4 mL of plasma and cfDNA was isolated using the QIAamp Circulating Nucleic Acid Kit (Qiagen, Hilden, Germany). The concentration of cfDNA was determined using the Qubit dsDNA High Sensitivity Assay Kit (ThermoFisher Scientific, Waltham, MA, USA) and cfDNA fragment distribution for subset of samples was obtained using

the Agilent 2100 Bioanalyzer System. To avoid within-patient batch effects, we isolated plasma cfDNA and performed methylation analysis for all visits from each patient together.

cfMeDIP-seq protocol

The cfMeDIP-seq protocol utilized in this study was adapted from a previously published protocol optimized for cfDNA (39). Isolated cfDNA was first end-repaired and A-tailed using the KAPA HyperPrep kit (Roche, Mannheim, Germany), followed by adapter ligation with index adapters (Integrated DNA technologies). Each adapter-ligated cfDNA sample was then spiked with λ phage DNA (ThermoFisher Scientific) as filler DNA, as well as methylated and unmethylated control *Arabidopsis thaliana* (AT) DNA (Diagenode, Denville, NJ, USA) to bring the total DNA amount to 100ng. Prior to immunoprecipitation, 10% of this DNA is saved as input control. The Diagenode MagMeDIP and IPure v2 kits were utilized to enrich and purify methylated cfDNA. Prior to library amplification, qPCR quality checks were performed to ensure: (1) high specificity (>95%) for enrichment of methylated AT DNA over unmethylated AT DNA, and (2) appropriate adapter-ligation. This was followed by adapter-specific amplification of each MeDIP and input control library and gel size selection. All sequencing was performed on the Illumina HiSeq 2500 platform (50-bp single end reads).

Sequencing data pre-processing and differential methylation analysis

Raw sequencing data was aligned to hg19 reference genome using Burrows-Wheeler alignment (BWA version 0.7.6a, using ‘mem’ option with default settings, except using –M flag). Duplicated reads were marked by Picard tools (<https://broadinstitute.github.io/picard/>) and collapsed to allow only one copy of the reads from reads that have the same alignment position.

Reads mapped to the multiple locations were removed by applying alignment quality threshold (QA>5). As the sequencing data was single-end, the average DNA fragment length was evaluated for both cfMeDIP and input controls using self-correlation technique (56). For each library, the fragment coverage genomic profile was calculated using directional extension of all aligned reads with estimated average fragment length (175bp in our case) using an in-house BAM2WIG custom tool (M. Bilenky, unpublished, see <http://www.epigenomes.ca/tools-and-software>). Within-patient differential methylation analysis for all comparisons was performed using DMRHunter pipeline developed for cfDNA samples (**Supplemental Methods Section**).

Statistical analysis of mCRPC-associated DMRs

Differences in regions with overall increase (UP) versus decrease (DOWN) in methylation across all comparisons were analyzed using the Wilcoxon rank-sum test as part of the base package of R (v3.5.3). Spearman correlation analysis was performed using similar base packages. Receiver operating characteristic (ROC) curve analysis was performed using the pROC package (1.14.0). All data was visualized using the ggplots2 package (v 3.1) and heatmaps from the package ComplexHeatmap (1.2). Pathway analysis is described in **Supplemental Methods Section**.

List of abbreviations

Androgen deprivation therapy (ADT)

Androgen receptor (AR)

Circulating cell free DNA (cfDNA)

Cell-free methylated DNA immunoprecipitation and high-throughput sequencing (cfMeDIP-seq)

503 Differentially methylated CpG sites (DMCs)
 504 Differentially methylated regions (DMRs)
 505 Metastatic castration resistant prostate cancer (mCRPC)
 506 Neuroendocrine-CRPC (NE-CRPC)
 507 Prostate cancer (PCa)
 508 Prostate-specific antigen (PSA)
 509 Time to progression (TTP)

510

511 **Declarations**

512 **Ethics approval and consent to participate:** All patients in this study provided informed
 513 written consent in accordance with approved institutional Research Ethics Board protocols from
 514 University Health Network (UHN) and Sinai Health System (SHS). Progress updates were
 515 submitted and approved annually by respective Research Ethics Boards. The study was
 516 performed in accordance with the Declaration of Helsinki.

517

518 **Consent for publication:** No personal information for any patient is presented in this
 519 manuscript. According to REB approvals, each patient was assigned unique study identifiers,
 520 which are not linked to personal health information.

521

522 **Availability of data and materials:** All FASTQ and QC files will be made available in a public
 523 repository upon publication of this manuscript. Additional supplementary data files have also
 524 been included.

525

Competing interests: There are no financial or non-financial interests to be declared.

Funding: This study was supported by a Prostate Cancer Canada Movember Discovery Grant (D2014-10) and an Astellas Prostate Cancer Innovation Fund (2017) to B. Bapat.

Authors' contributions: B.B. designed the study for intra-patient comparison. A.M.J. designed the clinical study for patient recruitment and sample collection. P.H. provided sample size calculations required for recruitment. M.R.P. performed sample processing, cfMeDIP-seq library preparation, and data analysis. M.B. developed and executed the DMRHunter pipeline and along with M.H., assisted with analysis to interpret cfMeDIP-seq datasets. R.I. and G.D.B. performed pathway analysis. S.Y.S. and D.D.D.C. designed the cfMeDIP-seq protocol and assisted with optimization for this study design. A.M.J., N.E.F. and A.R.H. were involved in patient follow-up and interpretation of data in the context of clinicopathological parameters. M.R.P., M.B. and B.B. composed the manuscript with feedback from all co-authors involved.

Acknowledgements: We acknowledge the UHN Genitourinary clinic and Genitourinary Biobank for recruiting patients, collecting blood samples and for patient follow-up/data collection. All sequencing and initial data pre-processing was performed by the Princess Margaret Genomics Centre and the UHN Bioinformatics and HPC Core, Princess Margaret Cancer Centre, respectively. Differential methylation analysis was performed using the facilities provided by the Canada's Michael Smith Genome Sciences Centre (British Columbia Cancer Agency). We also acknowledge Shivani Kamdar (SHS/LTRI) for assisting with sample processing and for helping to edit this manuscript.

References

1. Bray F, Ferlay J, Soerjomataram I, Siegel RL, Torre LA, and Jemal A. Global cancer statistics 2018: GLOBOCAN estimates of incidence and mortality worldwide for 36 cancers in 185 countries. *CA Cancer J Clin.* 2018;68(6):394-424.
2. Global Burden of Disease Cancer C, Fitzmaurice C, Allen C, Barber RM, Barregard L, Bhutta ZA, Brenner H, Dicker DJ, Chimed-Orchir O, Dandona R, et al. Global, Regional, and National Cancer Incidence, Mortality, Years of Life Lost, Years Lived With Disability, and Disability-Adjusted Life-years for 32 Cancer Groups, 1990 to 2015: A Systematic Analysis for the Global Burden of Disease Study. *JAMA Oncology.* 2017;3(4):524-48.
3. Wong YN, Ferraldeschi R, Attard G, and de Bono J. Evolution of androgen receptor targeted therapy for advanced prostate cancer. *Nat Rev Clin Oncol.* 2014;11(6):365-76.
4. Sridhar SS, Freedland SJ, Gleave ME, Higano C, Mulders P, Parker C, Sartor O, and Saad F. Castration-resistant prostate cancer: from new pathophysiology to new treatment. *Eur Urol.* 2014;65(2):289-99.
5. Crawford ED, Petrylak D, and Sartor O. Navigating the evolving therapeutic landscape in advanced prostate cancer. *Urol Oncol.* 2017;35S(S1-S13).
6. Scher HI, Fizazi K, Saad F, Taplin ME, Sternberg CN, Miller K, de Wit R, Mulders P, Chi KN, Shore ND, et al. Increased survival with enzalutamide in prostate cancer after chemotherapy. *N Engl J Med.* 2012;367(13):1187-97.
7. Lortot Y, Miller K, Sternberg CN, Fizazi K, De Bono JS, Chowdhury S, Higano CS, Noonberg S, Holmstrom S, Mansbach H, et al. Effect of enzalutamide on health-related quality of life, pain, and skeletal-related events in asymptomatic and minimally symptomatic,

chemotherapy-naive patients with metastatic castration-resistant prostate cancer (PREVAIL):
 results from a randomised, phase 3 trial. *Lancet Oncol.* 2015;16(5):509-21.

8. de Bono JS, Logothetis CJ, Molina A, Fizazi K, North S, Chu L, Chi KN, Jones RJ, Goodman OB, Jr., Saad F, et al. Abiraterone and increased survival in metastatic prostate cancer. *N Engl J Med.* 2011;364(21):1995-2005.

9. Ryan CJ, Smith MR, Fizazi K, Saad F, Mulders PF, Sternberg CN, Miller K, Logothetis CJ, Shore ND, Small EJ, et al. Abiraterone acetate plus prednisone versus placebo plus prednisone in chemotherapy-naive men with metastatic castration-resistant prostate cancer (COU-AA-302): final overall survival analysis of a randomised, double-blind, placebo-controlled phase 3 study. *Lancet Oncol.* 2015;16(2):152-60.

10. Bambury RM, and Scher HI. Enzalutamide: The story of its development from bench to bedside. *Urol Oncol.* 2015.

11. Grist E, de Bono JS, and Attard G. Targeting extra-gonadal androgens in castration-resistant prostate cancer. *J Steroid Biochem Mol Biol.* 2015;145(157-63.

12. Sumanasuriya S, and De Bono J. Treatment of Advanced Prostate Cancer-A Review of Current Therapies and Future Promise. *Cold Spring Harb Perspect Med.* 2018;8(6).

13. Fizazi K, Tran N, Fein L, Matsubara N, Rodriguez-Antolin A, Alekseev BY, Ozguroglu M, Ye D, Feyerabend S, Protheroe A, et al. Abiraterone plus Prednisone in Metastatic, Castration-Sensitive Prostate Cancer. *N Engl J Med.* 2017;377(4):352-60.

14. James ND, de Bono JS, Spears MR, Clarke NW, Mason MD, Dearnaley DP, Ritchie AWS, Amos CL, Gilson C, Jones RJ, et al. Abiraterone for Prostate Cancer Not Previously Treated with Hormone Therapy. *N Engl J Med.* 2017;377(4):338-51.

15. Armstrong AJ, Szmulewitz RZ, Petrylak DP, Holzbeierlein J, Villers A, Azad A, Alcaraz A, Alekseev B, Iguchi T, Shore ND, et al. ARCHES: A Randomized, Phase III Study of Androgen Deprivation Therapy With Enzalutamide or Placebo in Men With Metastatic Hormone-Sensitive Prostate Cancer. *J Clin Oncol*. 2019;JCO1900799.
16. Robinson D, Van Allen EM, Wu YM, Schultz N, Lonigro RJ, Mosquera JM, Montgomery B, Taplin ME, Pritchard CC, Attard G, et al. Integrative clinical genomics of advanced prostate cancer. *Cell*. 2015;161(5):1215-28.
17. Wyatt AW, Annala M, Aggarwal R, Beja K, Feng F, Youngren J, Foye A, Lloyd P, Nykter M, Beer TM, et al. Concordance of Circulating Tumor DNA and Matched Metastatic Tissue Biopsy in Prostate Cancer. *J Natl Cancer Inst*. 2017;109(12).
18. Morrison GJ, and Goldkorn A. Development and Application of Liquid Biopsies in Metastatic Prostate Cancer. *Curr Oncol Rep*. 2018;20(4):35.
19. Liu W, Yin B, Wang X, Yu P, Duan X, Liu C, Wang B, and Tao Z. Circulating tumor cells in prostate cancer: Precision diagnosis and therapy. *Oncol Lett*. 2017;14(2):1223-32.
20. Heller G, McCormack R, Kheoh T, Molina A, Smith MR, Dreicer R, Saad F, de Wit R, Aftab DT, Hirmand M, et al. Circulating Tumor Cell Number as a Response Measure of Prolonged Survival for Metastatic Castration-Resistant Prostate Cancer: A Comparison With Prostate-Specific Antigen Across Five Randomized Phase III Clinical Trials. *J Clin Oncol*. 2018;36(6):572-80.
21. Bastos DA, and Antonarakis ES. CTC-derived AR-V7 detection as a prognostic and predictive biomarker in advanced prostate cancer. *Expert Rev Mol Diagn*. 2018;18(2):155-63.
22. Scher HI, Graf RP, Schreiber NA, Jayaram A, Winquist E, McLaughlin B, Lu D, Fleisher M, Orr S, Lowes L, et al. Assessment of the Validity of Nuclear-Localized Androgen Receptor

616 Splice Variant 7 in Circulating Tumor Cells as a Predictive Biomarker for Castration-Resistant
617 Prostate Cancer. *JAMA Oncol.* 2018.

618 23. Antonarakis ES, Lu C, Luber B, Wang H, Chen Y, Zhu Y, Silberstein JL, Taylor MN,
619 Maughan BL, Denmeade SR, et al. Clinical Significance of Androgen Receptor Splice Variant-7
620 mRNA Detection in Circulating Tumor Cells of Men With Metastatic Castration-Resistant
621 Prostate Cancer Treated With First- and Second-Line Abiraterone and Enzalutamide. *J Clin*
622 *Oncol.* 2017;35(19):2149-56.

623 24. Millner LM, Linder MW, and Valdes R, Jr. Circulating tumor cells: a review of present
624 methods and the need to identify heterogeneous phenotypes. *Ann Clin Lab Sci.* 2013;43(3):295-
625 304.

626 25. Bernemann C, Schnoeller TJ, Luedeke M, Steinestel K, Boegemann M, Schrader AJ, and
627 Steinestel J. Expression of AR-V7 in Circulating Tumour Cells Does Not Preclude Response to
628 Next Generation Androgen Deprivation Therapy in Patients with Castration Resistant Prostate
629 Cancer. *Eur Urol.* 2016.

630 26. Takeuchi T, Okuno Y, Hattori-Kato M, Zaitzu M, and Mikami K. Detection of AR-V7
631 mRNA in whole blood may not predict the effectiveness of novel endocrine drugs for castration-
632 resistant prostate cancer. *Res Rep Urol.* 2016;8(21-5).

633 27. Beltran H, Prandi D, Mosquera JM, Benelli M, Puca L, Cyrta J, Marotz C, Giannopoulou
634 E, Chakravarthi BV, Varambally S, et al. Divergent clonal evolution of castration-resistant
635 neuroendocrine prostate cancer. *Nat Med.* 2016;22(3):298-305.

636 28. Corcoran RB, and Chabner BA. Application of Cell-free DNA Analysis to Cancer
637 Treatment. *N Engl J Med.* 2018;379(18):1754-65.

29. Ritch E, and Wyatt AW. Predicting therapy response and resistance in metastatic prostate cancer with circulating tumor DNA. *Urol Oncol*. 2017.
30. Romanel A, Tandefelt DG, Conteduca V, Jayaram A, Casiraghi N, Wetterskog D, Salvi S, Amadori D, Zafeiriou Z, Rescigno P, et al. Plasma AR and abiraterone-resistant prostate cancer. *Sci Transl Med*. 2015;7(312):312re10.
31. Azad AA, Volik SV, Wyatt AW, Haegert A, Le Bihan S, Bell RH, Anderson SA, McConeghy B, Shukin R, Bazov J, et al. Androgen Receptor Gene Aberrations in Circulating Cell-Free DNA: Biomarkers of Therapeutic Resistance in Castration-Resistant Prostate Cancer. *Clin Cancer Res*. 2015;21(10):2315-24.
32. Yegnasubramanian S. Prostate cancer epigenetics and its clinical implications. *Asian Journal of Andrology*. 2016;18(4):549-58.
33. Massie CE, Mills IG, and Lynch AG. The importance of DNA methylation in prostate cancer development. *J Steroid Biochem Mol Biol*. 2017;166(1-15).
34. Kron K, Liu L, Trudel D, Pethe V, Trachtenberg J, Fleshner N, Bapat B, and van der Kwast T. Correlation of ERG expression and DNA methylation biomarkers with adverse clinicopathologic features of prostate cancer. *Clin Cancer Res*. 2012;18(10):2896-904.
35. Mahon KL, Qu W, Devaney J, Paul C, Castillo L, Wykes RJ, Chatfield MD, Boyer MJ, Stockler MR, Marx G, et al. Methylated Glutathione S-transferase 1 (mGSTP1) is a potential plasma free DNA epigenetic marker of prognosis and response to chemotherapy in castrate-resistant prostate cancer. *Br J Cancer*. 2014;111(9):1802-9.
36. Gordevicius J, Krisciunas A, Groot DE, Yip SM, Susic M, Kwan A, Kustra R, Joshua AM, Chi KN, Petronis A, et al. Cell-Free DNA Modification Dynamics in Abiraterone Acetate-Treated Prostate Cancer Patients. *Clin Cancer Res*. 2018;24(14):3317-24.

661 37. Zhao F, Olkhov-Mitsel E, van der Kwast T, Sykes J, Zdravic D, Venkateswaran V, Zlotta
662 AR, Loblaw A, Fleshner NE, Klotz L, et al. Urinary DNA Methylation Biomarkers for
663 Noninvasive Prediction of Aggressive Disease in Patients with Prostate Cancer on Active
664 Surveillance. *J Urol*. 2017;197(2):335-41.

665 38. Hendriks RJ, Dijkstra S, Smit FP, Vandersmissen J, Van de Voorde H, Mulders PFA, van
666 Oort IM, Van Criekinge W, and Schalken JA. Epigenetic markers in circulating cell-free DNA as
667 prognostic markers for survival of castration-resistant prostate cancer patients. *Prostate*. 2018.

668 39. Shen SY, Singhania R, Fehringer G, Chakravarthy A, Roehrl MHA, Chadwick D,
669 Zuzarte PC, Borgida A, Wang TT, Li T, et al. Sensitive tumour detection and classification using
670 plasma cell-free DNA methylomes. *Nature*. 2018;563(7732):579-83.

671 40. Kamdar SN, Ho LT, Kron KJ, Isserlin R, van der Kwast T, Zlotta AR, Fleshner NE,
672 Bader G, and Bapat B. Dynamic interplay between locus-specific DNA methylation and
673 hydroxymethylation regulates distinct biological pathways in prostate carcinogenesis. *Clin*
674 *Epigenetics*. 2016;8(32).

675 41. Baylin SB, and Jones PA. Epigenetic Determinants of Cancer. *Cold Spring Harb Perspect*
676 *Biol*. 2016;8(9).

677 42. Zeng T, Zhu L, Liao M, Zhuo W, Yang S, Wu W, and Wang D. Knockdown of PYCR1
678 inhibits cell proliferation and colony formation via cell cycle arrest and apoptosis in prostate
679 cancer. *Med Oncol*. 2017;34(2):27.

680 43. Yang F, Zhang Y, Ressler SJ, Ittmann MM, Ayala GE, Dang TD, Wang F, and Rowley
681 DR. FGFR1 is essential for prostate cancer progression and metastasis. *Cancer Res*.
682 2013;73(12):3716-24.

44. Manda KR, Tripathi P, Hsi AC, Ning J, Ruzinova MB, Liapis H, Bailey M, Zhang H, Maher CA, Humphrey PA, et al. NFATc1 promotes prostate tumorigenesis and overcomes PTEN loss-induced senescence. *Oncogene*. 2016;35(25):3282-92.
45. Wang R, Chen X, Xu T, Xia R, Han L, Chen W, De W, and Shu Y. MiR-326 regulates cell proliferation and migration in lung cancer by targeting phox2a and is regulated by HOTAIR. *Am J Cancer Res*. 2016;6(2):173-86.
46. Takayama K, Suzuki T, Fujimura T, Urano T, Takahashi S, Homma Y, and Inoue S. CtBP2 modulates the androgen receptor to promote prostate cancer progression. *Cancer Res*. 2014;74(22):6542-53.
47. Guo H, Ci X, Ahmed M, Hua JT, Soares F, Lin D, Puca L, Vosoughi A, Xue H, Li E, et al. ONECUT2 is a driver of neuroendocrine prostate cancer. *Nat Commun*. 2019;10(1):278.
48. Yang YA, Zhao JC, Fong KW, Kim J, Li S, Song C, Song B, Zheng B, He C, and Yu J. FOXA1 potentiates lineage-specific enhancer activation through modulating TET1 expression and function. *Nucleic Acids Res*. 2016;44(17):8153-64.
49. Mahon KL, Qu W, Lin HM, Spielman C, Cain D, Jacobs C, Stockler MR, Higano CS, de Bono JS, Chi KN, et al. Serum Free Methylated Glutathione S-transferase 1 DNA Levels, Survival, and Response to Docetaxel in Metastatic, Castration-resistant Prostate Cancer: Post Hoc Analyses of Data from a Phase 3 Trial. *Eur Urol*. 2018.
50. Brocks D, Assenov Y, Minner S, Bogatyrova O, Simon R, Koop C, Oakes C, Zucknick M, Lipka DB, Weischenfeldt J, et al. Intratumor DNA methylation heterogeneity reflects clonal evolution in aggressive prostate cancer. *Cell Reports*. 2014;8(3):798-806.
51. Aryee MJ, Liu W, Engelmann JC, Nuhn P, Gurel M, Haffner MC, Esopi D, Irizarry RA, Getzenberg RH, Nelson WG, et al. DNA methylation alterations exhibit intraindividual stability

and interindividual heterogeneity in prostate cancer metastases. *Sci Transl Med*. 2013;5(169):169ra10.

52. Friedlander TW, Roy R, Tomlins SA, Ngo VT, Kobayashi Y, Azameera A, Rubin MA, Pienta KJ, Chinnaiyan A, Ittmann MM, et al. Common structural and epigenetic changes in the genome of castration-resistant prostate cancer. *Cancer Res*. 2012;72(3):616-25.

53. Huang H, Du T, Zhang Y, Lai Y, Li K, Fan X, Zhu D, Lin T, Xu K, Huang J, et al. Elevation of SHARPIN Protein Levels in Prostate Adenocarcinomas Promotes Metastasis and Impairs Patient Survivals. *Prostate*. 2017;77(7):718-28.

54. Zhang D, Park D, Zhong Y, Lu Y, Rycak K, Gong S, Chen X, Liu X, Chao HP, Whitney P, et al. Stem cell and neurogenic gene-expression profiles link prostate basal cells to aggressive prostate cancer. *Nat Commun*. 2016;7(10798).

55. Hara I, Yamashita S, Nishizawa S, Kikkawa K, Shimokawa T, and Kohjimoto Y. Enzalutamide Versus Abiraterone as a First-Line Endocrine Therapy for Castration-Resistant Prostate Cancer: Protocol for a Multicenter Randomized Phase 3 Trial. *JMIR Res Protoc*. 2018;7(7):e11191.

56. Ramachandran P, Palidwor GA, Porter CJ, and Perkins TJ. MaSC: mappability-sensitive cross-correlation for estimating mean fragment length of single-end short-read sequencing data. *Bioinformatics*. 2013;29(4):444-50.

Figure Legends

Figure 1. Within patient differential methylation analysis strategy to monitor temporal changes in cfDNA.

In order to help identify methylation changes associated with treatment in cfDNA, we opted to perform within-patient methylation analysis to identify differentially methylated regions (DMRs) associated with tumor response and/or resistance to current treatments. Each patient in this study received either Enzalutamide or Abiraterone acetate and blood was collected prior to initiating therapy (**Visit A**), at 12-weeks during treatment (**Visit B**) and upon clinical progression/treatment change (**Visit C**). We applied an established genome-wide method to detect methylated cfDNA fragments followed by extensive analysis to identify DMRs associated with treatment response. We compared all study visits available (Visit B vs A, C vs B, and C vs A) to find losses or gains in methylated cfDNA fragments. For instance, loss of treatment responsive tumor cells (green methylated DNA fragments at visit B) or gains in treatment insensitive/resistant tumor cells (blue DNA fragments at visit C) could be detected with this strategy.

Figure 2. Sample collection and patient clinical follow-up overview.

(a) Plasma samples from mCRPC patients receiving Enzalutamide (12 patients) or Abiraterone acetate (4 patients) were collected at baseline (Visit A), at week-12 (+/- 2 weeks, Visit B) and upon clinical progression (Visit C). The total number of samples collected at each visit is shown. 2 Enzalutamide-treated patients (P2 and P26) were unable to provide samples for Visit C and 1 Abiraterone-treated patient (P36) progressed prior to Visit B. For these patients, the date of treatment change/clinical progression was recorded for data analysis. (b) Pie chart summarizes

the distribution of metastasis locations at mCRPC diagnosis. (c) Bar plot shows best PSA response for each patient during treatment (nadir), expressed as a percentage of Baseline/Visit A PSA. Dotted line indicates $\geq 50\%$ decline in PSA from Visit A. (d) Overall timeline of study follow-up starting from Visit A to Visit C/Final visit is shown for all patients. Green dots represent Visit B, red dots are Visit C or final study visit (if Visit C was not collected), yellow indicates lowest PSA level (nadir) and blue dots show first PSA rise during treatment.

Figure 3. Summary of intra-patient DMR analysis.

(a) The total number of DMRs for all patients, visit comparison and treatment. (b) Boxplot summarizing median, first and third quartile of all comparison DMRs. Whiskers represent the highest and lowest number of DMRs. (c) DMR totals were further stratified by treatment type. Boxplots illustrate percentage of DMRs that increased or decreased in methylation in (d) B vs A, (e) C vs B and (f) C vs A. (g) The overall proportion of DMRs that were identified near/within CGI, shore, TSS/promoter, ncRNA, intergenic and gene body regions is shown for all visit comparisons (In order of B vs A, C vs B and C vs A). (h) Venn diagrams showing the overlap of protein coding genes with DMRs near their promoters is shown for all visit comparisons and between Enzalutamide- and Abiraterone-treated patients. (i) Similarly, the overlap of protein coding regions with DMRs within gene bodies is shown.

Figure 4. Key prostate cancer related methylation changes observed in cfDNA

(a) Heatmap shows methylation trends in promoter regions for all patients and comparisons of the most frequently methylated genes in PCa. For each gene, the proportion of DMRs with increased (blue) and decreased (red) methylation was calculated and the net change is shown.

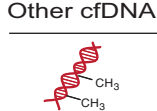
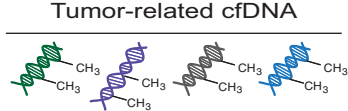
Grey indicates no net change in methylation. Representative peaks show methylation levels (normalized read counts) of (b) *GSTP1* (black dotted lines indicating gene body) and (c) *TBX15*. LNCaP cell line MeDIP-seq data is also shown.

Figure 5. Common differentially methylated CpGs (DMCs).

(a) For patients that were able to provide samples for all three visits, the proportion of CpG sites that were differentially methylated in a single comparison and shared across 2 or more comparisons is shown. 14 possible scenarios are represented by different colors. TTP in weeks are also indicated for each patient. (b) Spearman correlation analysis of the proportion of DMCs that were found to increase or decrease in B/C vs A (scenarios 9 & 10) against time to progression (Spearman rho and p values are shown).

Figure 6. NE-CRPC related DMRs in cfDNA.

(a) For each patient, the proportion of DMRs that demonstrated methylation differences in NE-CRPC associated regions in visit A vs B. (b) For DMRs that contained NE-CRPC associated CpGs, various FDR thresholds were applied to assess for optimal regions that correlated with TTP. (c) Using the optimal FDR cut-off, the ratio of NE-associated DMRs with increased methylated fragments in visit A vs B to decreased fragments was correlated with TTP (Spearman rho and p value is shown). For P36, A vs C comparison was used as this patient progressed prior to visit B. (d) ROC analysis shows optimal AUC (0.927, 95% CI: 0.773-1) that stratifies patients according to TTP (<25 weeks).



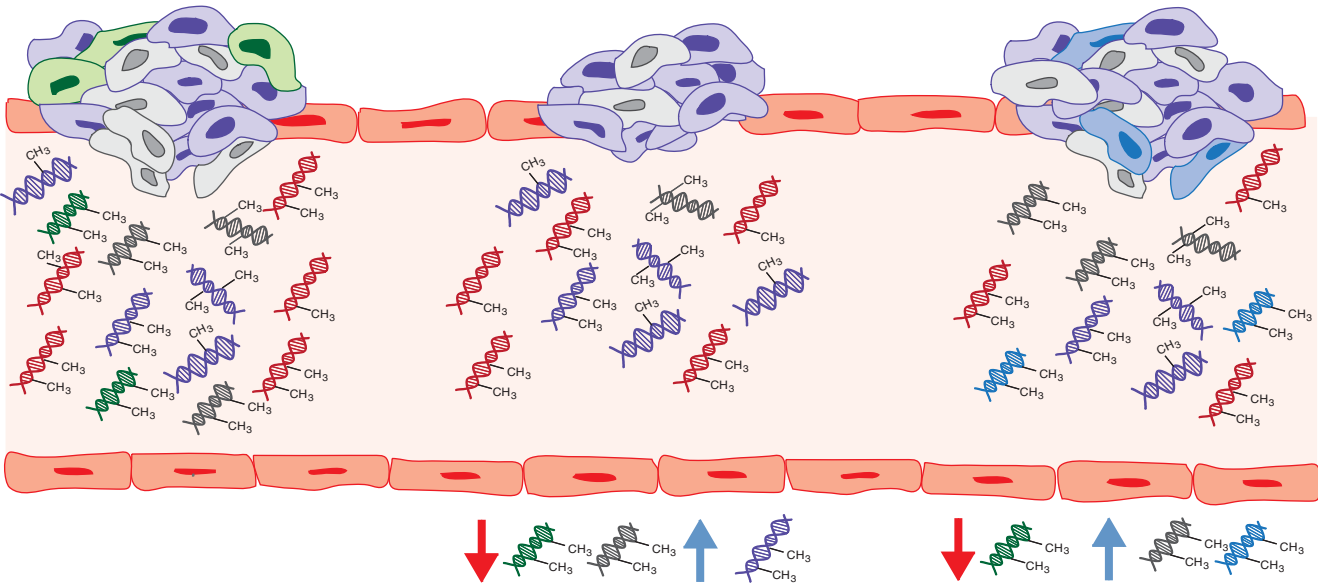
Down: Loss/Reduction of methylated cfDNA fragment
Source: Treatment responsive cells

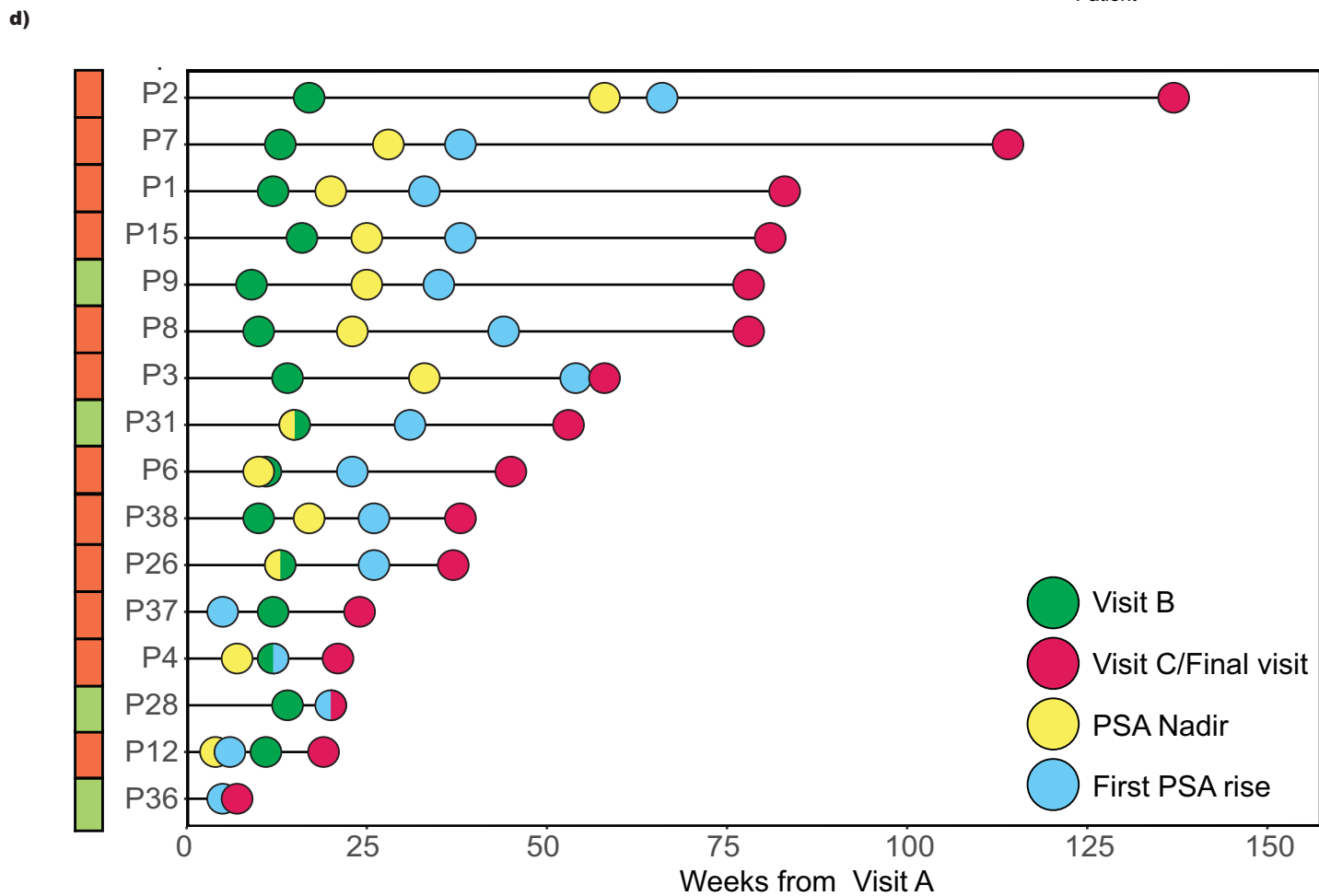
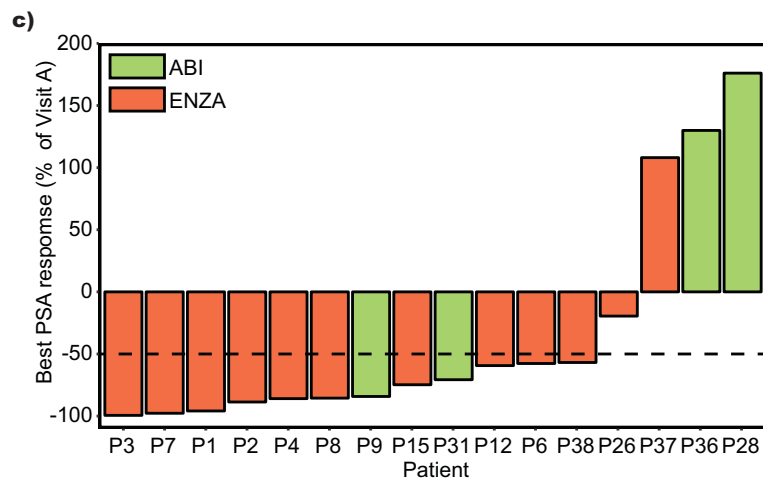
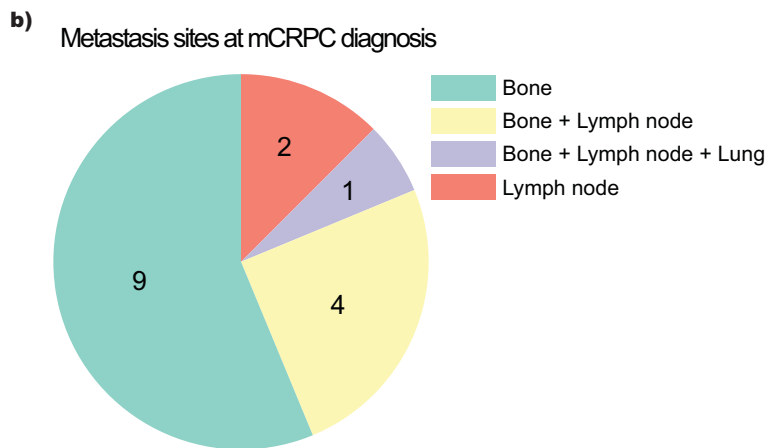
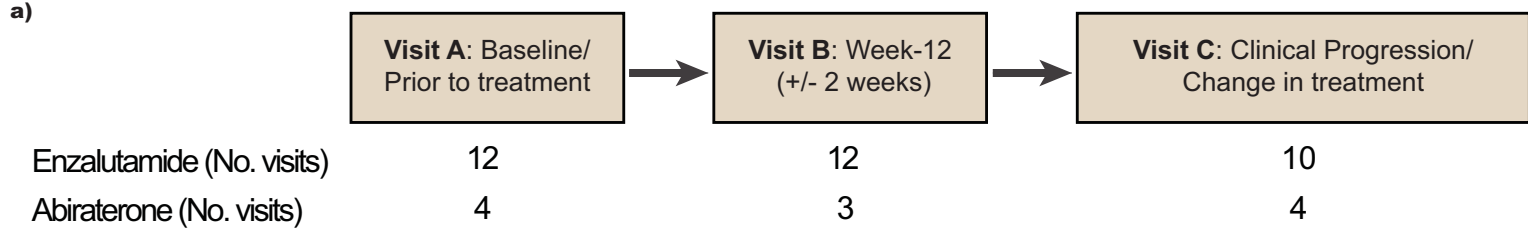
UP: Gain/Increase of methylated cfDNA fragment
Source: Treatment resistant cells

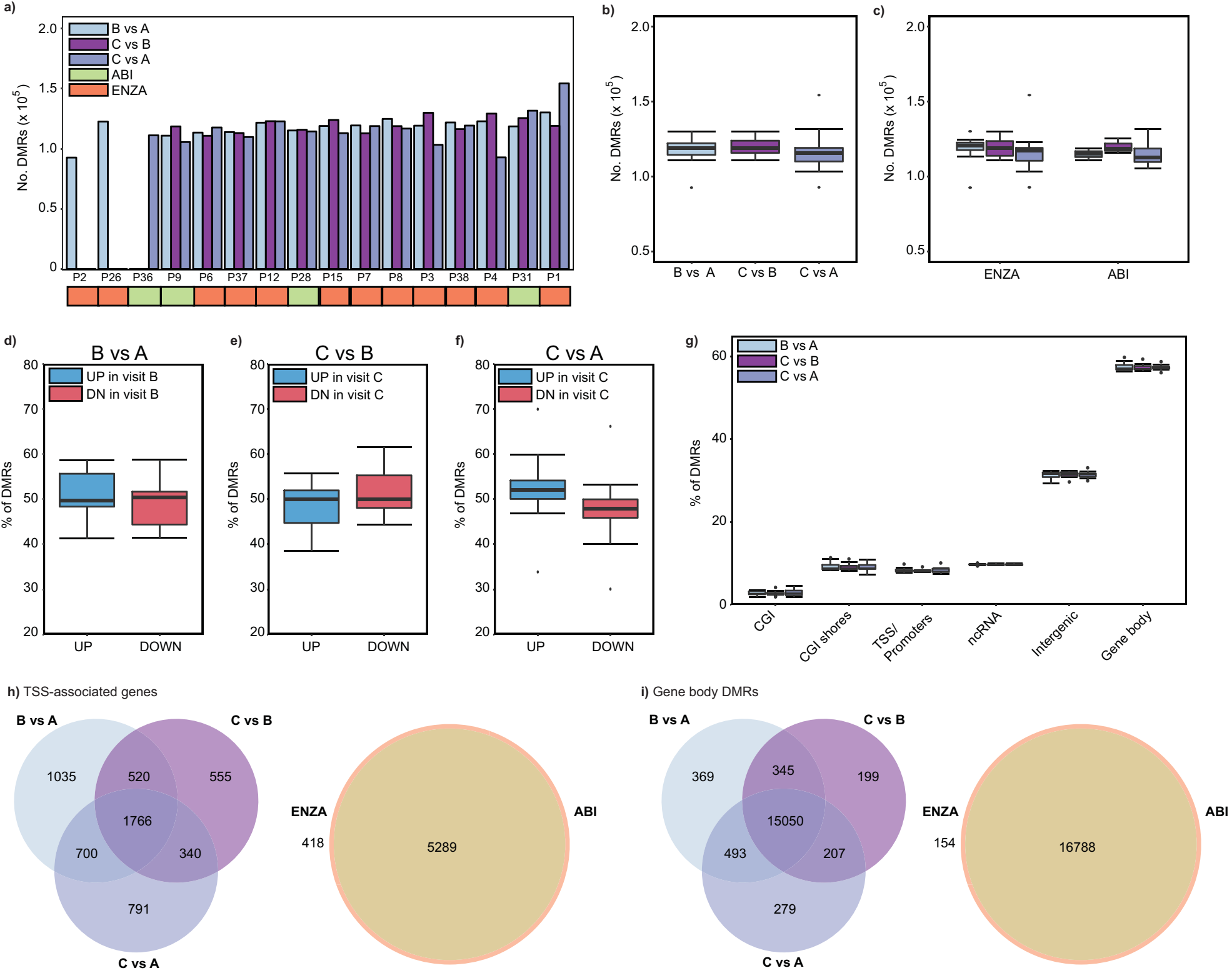
Visit A: Baseline

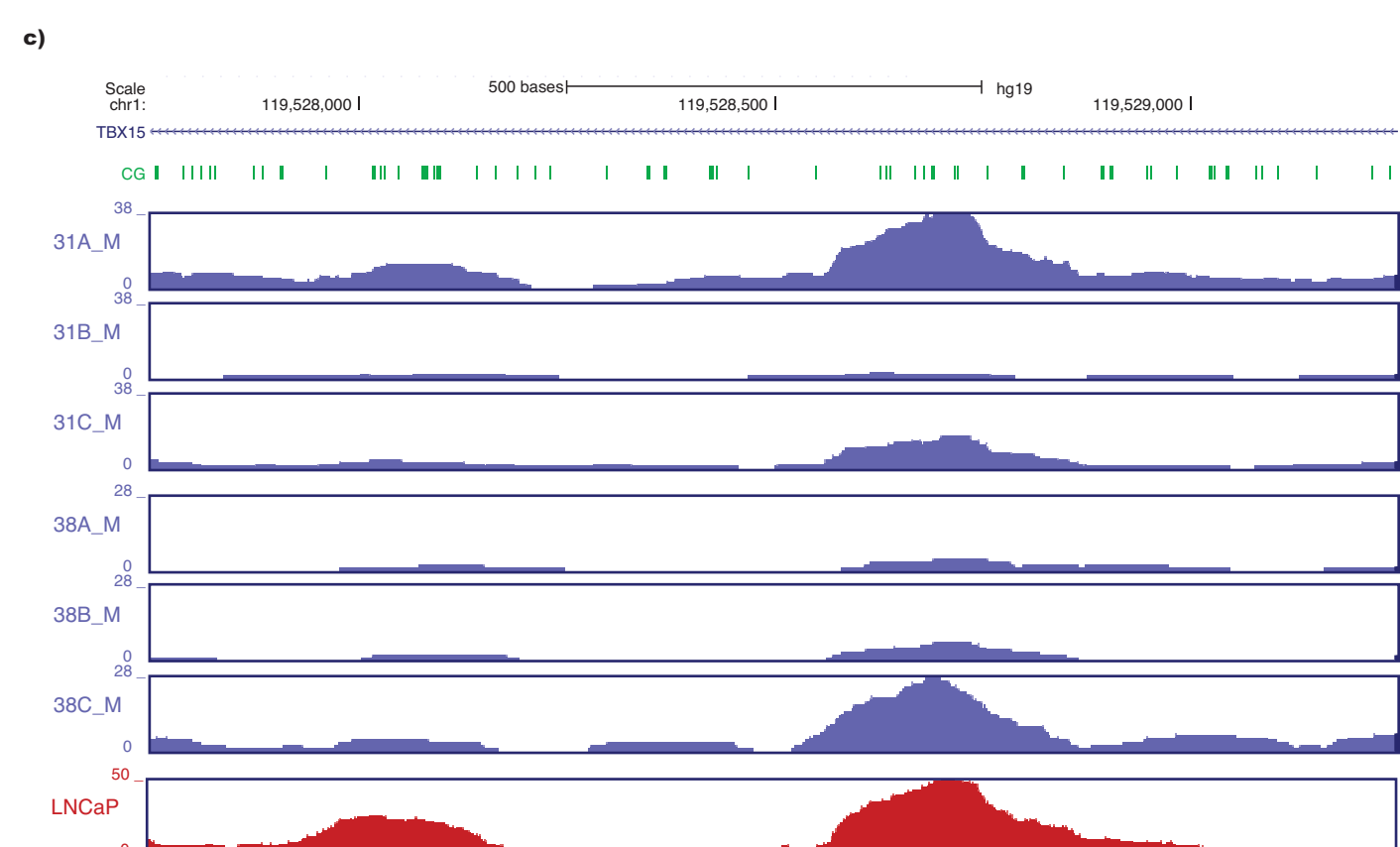
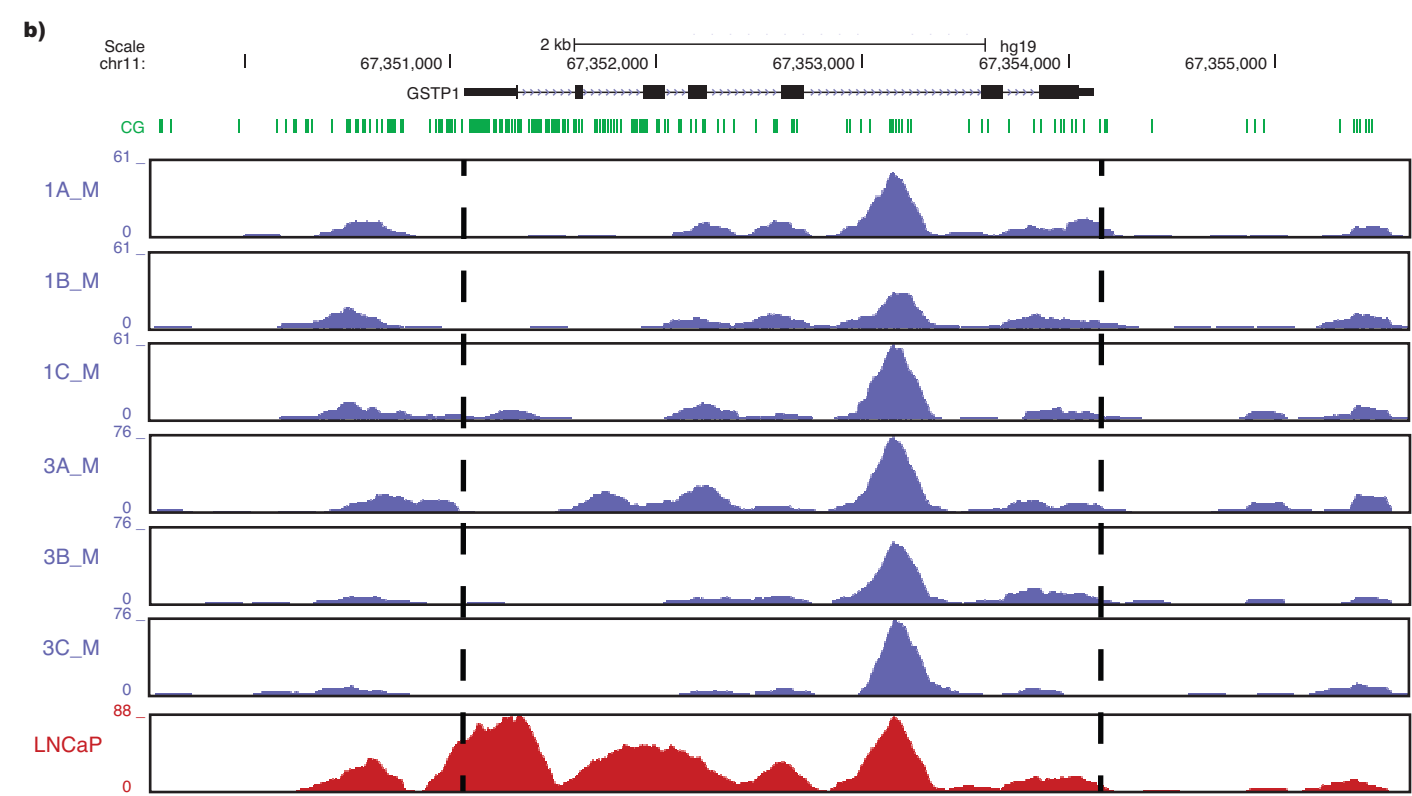
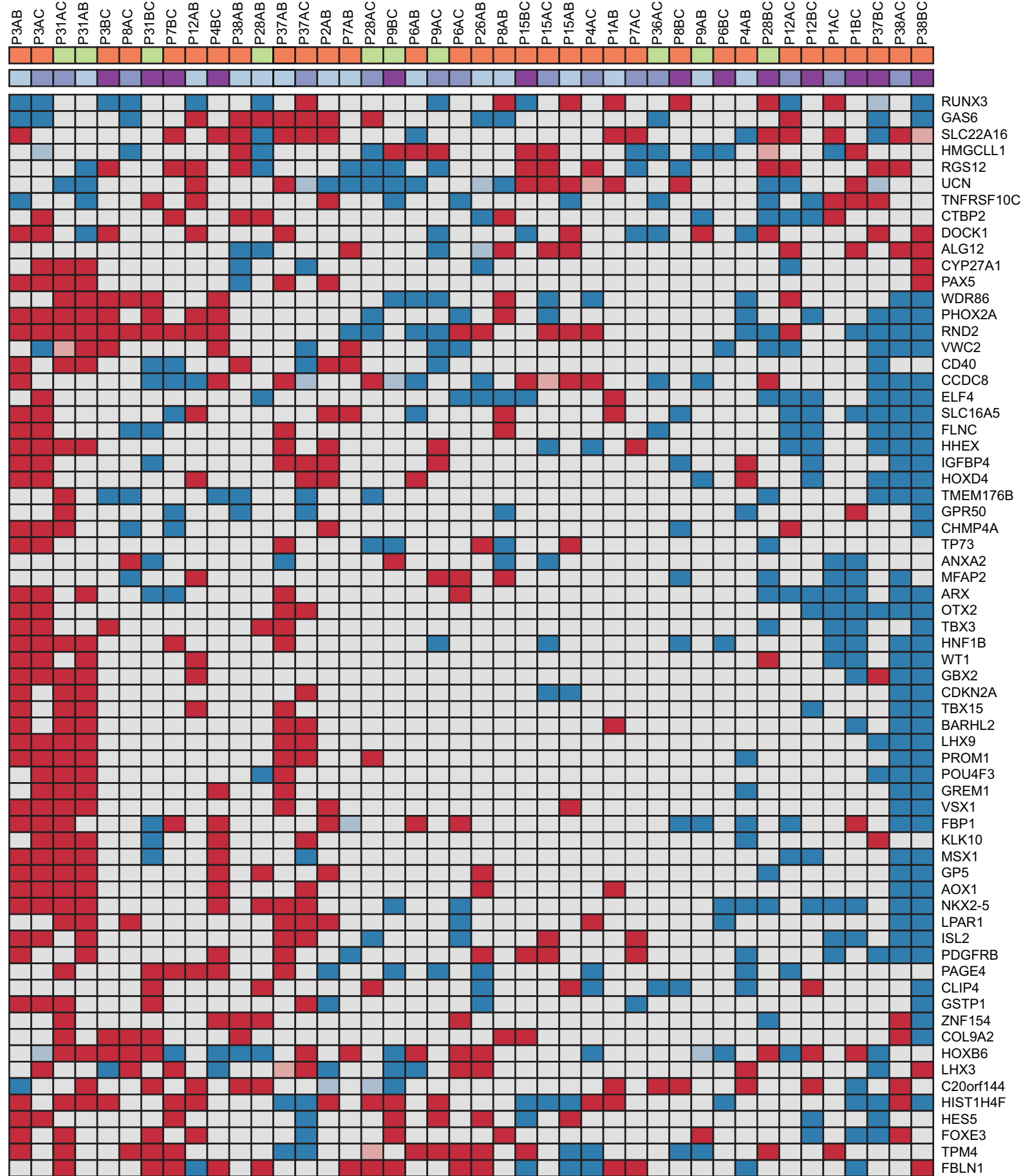
Visit B: Week-12

Visit C: Clinical Progression



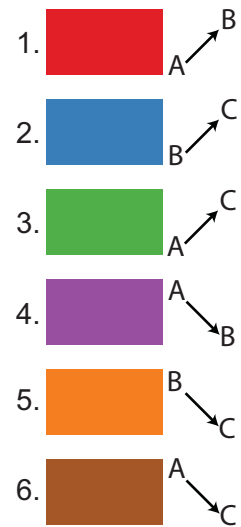




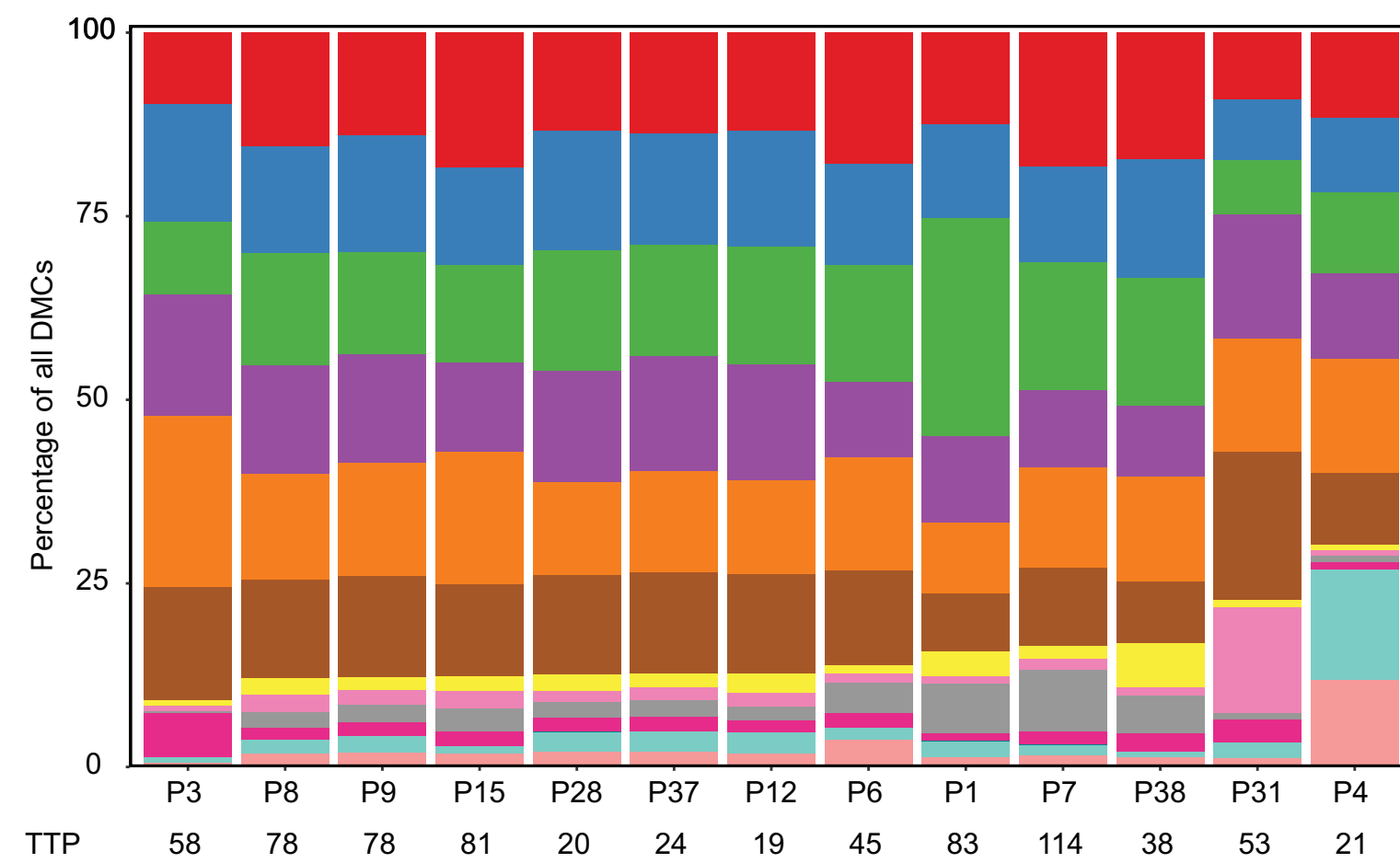
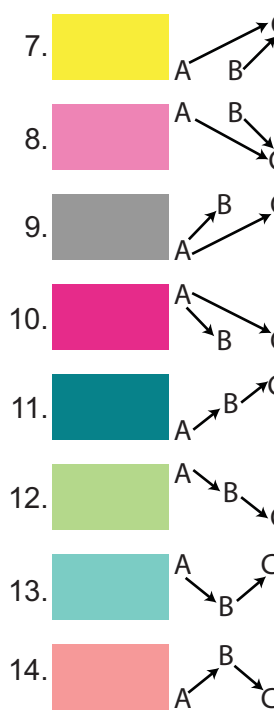


a)

DMCs in single visit comparisons



DMCs shared across comparisons



b)

Percentage of all DMCs

